Aspects of Muonium Chemistry

Tom A. Claxton
Department of Chemistry, Leicester University, Leicester, LE1 7RH, U.K.

1 Introduction

1937 was marked by the birth of the author and the discovery of the muon, although another 10 years were required for positive proof of the latter. But it was not until 1957 when chemists should have shown any interest, with the discovery of muonium, a bound state between a positive muon, μ^+, and an electron, which is commonly referred to as a pseudo-isotope ($m_\mu = \frac{1}{9} m_H$) of the hydrogen atom. Actually the negatively charged muon also exists but its analogy to a heavy electron (*ca.* $200m_e$) has not been put to use by chemists. The unexpected rise to fame in chemistry of this unexpected fundamental particle must be associated with the easy formation of muonium and its subsequent reactions. But this is too glib; really its success arises from two facts: firstly the muon polarisation at production is preserved and secondly this polarisation direction at decay is the preferred direction of the ejected positron. In other words it has a special signature which not only allows its presence to be observed but also acts as a unique probe to give information about its molecular environment. Although it is not our concern here to discuss experimental details, some observations on the two facts above are necessary to appreciate the advantages and limitations of the technique. For instance the experiment can be carried out in the absence of external magnetic fields (zero field), or with a magnetic field parallel (longitudinal field) or perpendicular (transverse field) to the beam direction (muon polarisation).

A remarkable feature of μSR spectroscopy is that the ionising particle is itself studied. This contrasts with other fields of radiation chemistry. In view of the light mass of the muon, damage to the target material is slight, although some (ionisation) is necessary to form muonium (see next section) which is so crucial to chemistry. In many cases the region round its terminal track will be well removed from this damage enabling study of chemical reaction with undamaged material.

There are a number of recent reviews on muon as a probe in physics[1] and chemistry.[2] Here focus is made on some recent topics for which theoretical methods have been particularly helpful, although the emphasis will remain qualitative throughout.

2 Muonium

First of all we need to discuss how a muon spin interacts with an electron spin in the simplest system, muonium. From our point of view muon spin differs from a proton spin only in the magnitude of its magnetic moment, $\mu_\mu = 3.18334\mu_p$, with similar 'up' and

Tom Claxton obtained a B.Sc. from University College London in 1958 and continued there for a Ph.D. with David Craig, FRS. After post-doctoral work at NRC, Ottawa, Canada with Cam Benson he took up a position at Leicester University in 1963 where he is now a Senior Lecturer. His early theoretical work on radicals observed by ESR has increasingly been replaced with those observed by μSR.

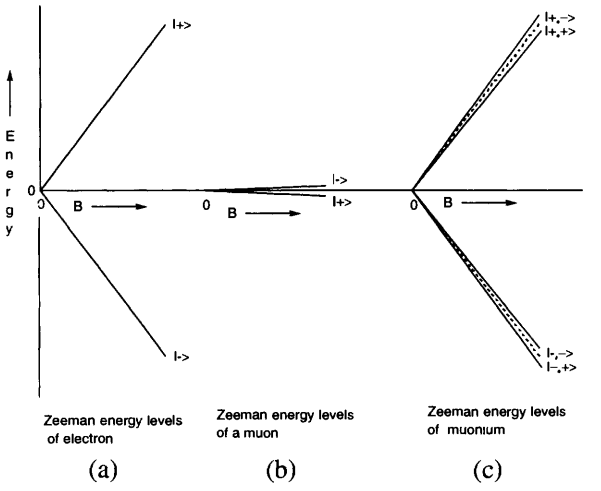

Figure 1 Zeeman splitting.

'down' spin states loosely labelled here as $|+\rangle$ and $|-\rangle$. The energy of the $|+\rangle$ spin state is lowered, by an amount proportional to the externally applied magnetic field, $\boldsymbol{B}$, by the same amount that the $|-\rangle$ spin state is raised. These are the muon Zeeman levels. Perversely the electron, also with two spin states $|+\rangle$ and $|-\rangle$ but with a considerably larger magnetic moment ($\mu_e = 206.8\mu_\mu$), does the opposite, that is, it has its $|+\rangle$ spin state raised by the same amount as the $|-\rangle$ spin state is lowered. Since these energy changes are also proportional to the magnetic moments it is clear that the electron Zeeman energy levels are split by a factor of over 200 compared to the muon spin, as shown qualitatively in Figures 1a and 1b. (If that figure were drawn true to scale the muon Zeeman states would be indistinguishable). To discuss the muon–electron pair each state is written in the style $|+,-\rangle$ where the first descriptor, + here, refers to the electron and the second descriptor, − here, refers to the muon.

This basically additive process (Figure 1c) neglects the magnetic interaction (or the hyperfine coupling constant, A, is assumed to be zero) between the two spins. Crudely the magnetism associated with the muon spin will interact with the magnetism associated with the electron spin, just like two bar magnets. When separated this gives rise to the anisotropic component (which averages to zero if the pair are tumbling freely) but when superimposed (the so-called Fermi contact term when an electron 'sits' on the nucleus) this constitutes the isotropic component (which is not averaged by a tumbling motion and is independent of the external field). For sufficiently high magnetic fields ($g\beta B/h >> A$) (> 2 T for muonium, but only > 0.3 T for many organic radicals because of the smaller coupling constants) this spin–spin interaction is too weak to disturb significantly the alignment of the spins with the external magnetic field and it is sufficient just to add the hyperfine interaction to each Zeeman level. If the two spins are parallel the interaction will be in the opposite sense than when the two spins are opposed (the term is $A\boldsymbol{I}.\boldsymbol{S}$) so if the electron spin is in the same direction as the muon spin the contribution will be proportional to A but to $-A$ for opposing spins. A can be positive or negative, as is well known in ESR. For convenience of construction (Figure 2), but by no means correct at zero or small magnetic fields, the hyperfine coupling interaction, A, is considered first and then the effect of the Zeeman interaction (energy of the nuclear magnetic dipoles in the magnetic field, $\boldsymbol{B}$, i.e. $-2\pi\boldsymbol{B}\sum_i m_z^i\gamma_i$, where m_z^i is either +½ or −½

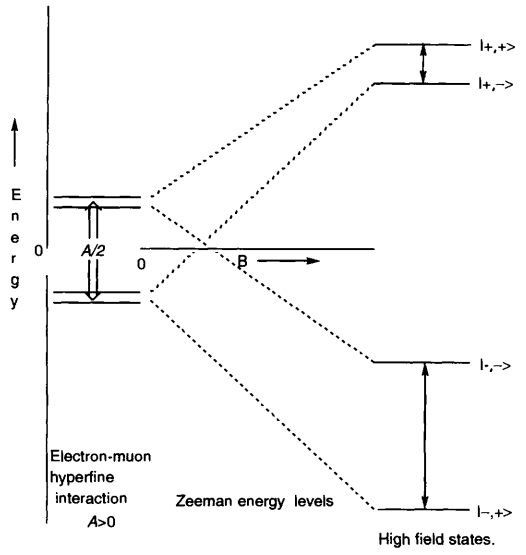

Figure 2 Zeeman and hyperfine interactions in muonium.

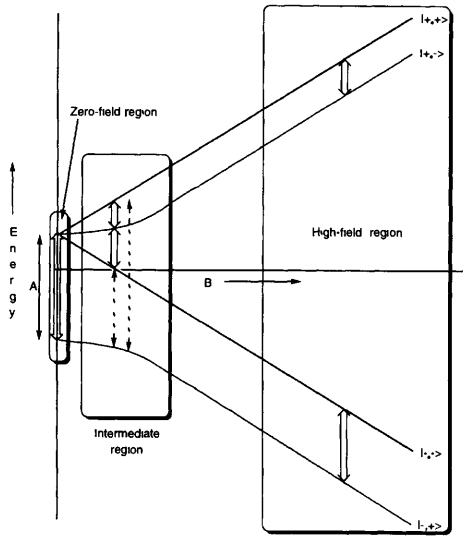

Figure 3 Breit-Rabi diagram for an electron and a nucleus ($I = ½$) ignoring nuclear Zeeman interaction. The labelling of the spin states in the high-field region does not hold in the other regions.

for particle i with ½-spin and γ_i is the corresponding gyromagnetic ratio) is included. The final energy levels (to the right of the diagram) are correct at sufficiently high magnetic field.

In fact A is positive in muonium and Figure 2 correlates with the quantitative Breit–Rabi diagram in the high-field regime (Figure 3) which shows the lower two levels to be more widely split than the upper two. The allowed transitions involving a 'flip' of the muon spin are indicated explaining the observation of two resonances in the spectrum separated by the hyperfine coupling constant, A. The differences with the Breit–Rabi diagram, which occur at zero and small magnetic fields are important. These involve the $|+,-\rangle$ and $|-,+\rangle$ states because without the large difference in Zeeman interaction the spins become essentially identical in character and mix to form the singlet and triplet combinations, just like the proton spins in H_2 or the unpaired electrons in the oxygen molecule.

The zero-field region is where the magnetic (field-independent) interaction is the only magnetic field affecting the spins. This gives rise to the singlet/triplet state description, the separation of the singlet and triplet levels actually being proportional to the magnetic interaction A. The intermediate region, where the external magnetic field is of the order of the magnetic interaction, can only be dealt with quantitatively. Dominant transitions are indicated using double arrows as ⇔ while dotted arrows indicate transitions which can only be observed with difficulty.

Although the description here could appear in any article on magnetic resonance there is a significant difference in the μSR experiment; the transitions in conventional magnetic resonance experiments require an inducing RF field whereas they appear spontaneously in μSR. This will be explained next.

3 Muon Detection

Muons, μ^+, are a decay product from pions.

$$\pi^+ \rightarrow \mu^+ + \nu_\mu$$

Conservation of angular momentum ensures that the muons can be produced with all their spins polarised longitudinally along the beam (Figure 4a), a polarisation which tends to be preserved through the whole process of thermalisation (dissipation of the

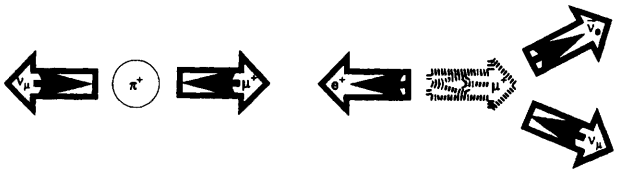

Figure 4 (a) Decay of pion. (b) Decay of muon. ⇢ represents the momentum vector. ➛ represent the particle spin or neutrino helicity vectors.

beam energy by collisions *etc.*) and implantation (eventual trapping in the material either by chemical combination or trapping in a lattice). The fact that it can be assumed that the polarisation is preserved during reactions of chemical interest is crucial to the success of the technique. The lifetime of the muon is 2.2 μs. When it decays it does so according to the scheme:

$$\mu^+ \rightarrow e^+ + \bar{\nu}_e + \nu_\mu$$

where the positron, e^+, is of particular interest. Although the electron antineutrino and muon neutrino are not monitored they are important to the success of the experiment.

As shown in Figure 4b the positron is ejected preferentially along the polarisation direction of the muon providing a suitable means of monitoring the muon spin direction at its moment of decay. Given this good basis for detection much of the rest of the technique has depended on the ingenuity of the experimentalists, sometimes borrowing ideas from nuclear magnetism in general, and similarities of various techniques to ENDOR and pulsed NMR methods are very evident. Here we discuss only the most common μSR methods, muon spin resonance and muon spin rotation (both using the same acronym μSR) just to illustrate the techniques and to emphasise differences with conventional magnetic resonance experiments.

3.1 Muon Spin Relaxation

In a longitudinal field, strong enough to quench competing local fields, muons are implanted in a stationary state with the initial polarisation being preserved. Relaxation of the muon Zeeman energy [measured by monitoring the number of ejected positrons (Figure 5) on both sides of the sample along the beam, that is, measuring the polarisation in the forward and backward directions] is analogous to the T_1 relaxation familiar in NMR. By varying the longitudinal field, the minium field, $\boldsymbol{B}_{min}$, necessary to recover the polarisation (that is quench or decouple the muon–electron hyperfine coupling or superhyperfine interactions to other nuclei) may be the only clue to the existence of a chemically involved muon. At least it is usually possible to distinguish between a chemically involved muon and one where the polarisation has been lost due to spin-exchange reaction or spin-flip encounters with other paramagnetic species. If the latter processes are important the polarisation is irretrievably lost. This applies to the transverse fields, discussed below, as well. The worst common offender here is molecular oxygen and explains why great efforts are made to remove oxygen from gas or liquid target materials.

The general selection rule for transitions in a longitudinal field is that there cannot be a change ($\Delta M = 0$) in the component of the total spin in the field direction, $M = m_\mu + m_e + m_N$, where m_N is a spin component of a spin ½ nucleus, N, for which there is a superhyperfine interaction with the muon *via* the electrons Abragam[3] pointed out that where degeneracies in the Zeeman levels were possible (points of level crossing) a highly enhanced resonant 'depolarisation' may occur leading to a very sensitive technique commonly referred to as 'Avoided Level Crossing' or ALC and explained in section 4

3.2 Muon Spin Rotation

Muons implanted in a sample placed in a strong transverse magnetic field (that is, perpendicular to the polarised beam) will precess about this external field with an appropriate Larmor frequency as illustrated in Figure 5b This is detectable because the decaying muon will eject a positron (Figure 5c) in its current orientation which can be picked up by a scintillator A particular detector will see 'flashes'

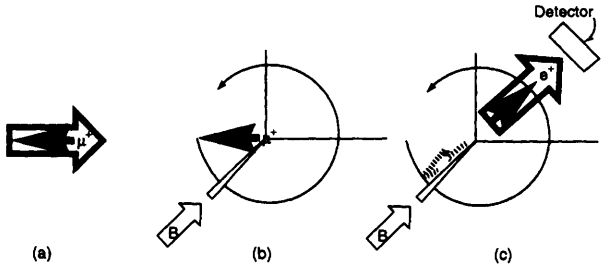

Figure 5 (a) Muon beam (b) Muon at rest in sample Magnetic field going into paper (c) Muon decays and ejects positron towards detector

of positrons with a period corresponding to the Larmor frequency More importantly, if there are also internal magnetic fields present, for example arising from an electron–muon hyperfine interaction as discussed above for muonium, the effective magnetic field will be different which will be seen as a different Larmor frequency All of this has to be done electronically and millions of events are recorded and analysed to obtain a μSR spectrum

There is another way of looking at this process which draws an analogy with pulsed NMR In a pulsed NMR experiment the sample is irradiated with an RF pulse of short duration which aligns all the nuclear spins along a fixed direction perpendicular to the static field and the change in magnetic polarisation is monitored In muon spin rotation there is no necessity to resort to RF pulses since the muons are already polarised along a known direction and if a magnetic field is applied perpendicular to this polarisation the analogy is complete So in the transverse field μSR experiment the muons are implanted in the sample in a non-stationary state, a coherent superposition of the two spin states

3.3 Relaxation and Rotation

Relaxation processes, for example, spin-exchange or spin-flip reactions, can be a serious hindrance in muon experiments and, as already indicated, great care is sometimes necessary to remove molecular oxygen from gases and liquids They can also be used, to good advantage, to investigate diffusion processes where both transverse and longitudinal fields give complementary results This was strikingly shown very recently[4] with the muonium–oxygen reaction being studied in liquid water It was shown to be dominated by electron spin exchange (*ca* 90%) The longitudinal field quenching experiment enables the spin-exchange reactions to be separated from the chemical reaction Analogous reactions have been carried out for both protium and deuterium using ESR providing an ideal system for determining the mass dependence, if any It was concluded that the diffusion coefficient of muonium was *twice* that of protium which is unprecedented since generally the diffusion coefficients of the 'true' isotopes of hydrogen depend on the inverse of the cube root of the mass It is also concluded that the chemical reaction of Mu with O_2 is not quite at the diffusion-control limit

4 Avoided Level Crossing Spectroscopy

4.1 Open Shell Systems

In ESR electron spin transitions are monitored which reflect, to first order, the extent that each nuclear spin interacts with the unpaired electron In μSR of paramagnetic species the muon spin transitions are monitored and, to first order, only reflect the interaction with the unpaired electron spin However this interaction will be affected by other nuclear spins since these will interact with and disturb the distribution of the unpaired electron and hence the electron–muon interaction, but the effect is small, and has only been observed at low transverse fields in very special cases

Continuing with a qualitative explanation of these effects it is convenient to modify the previous diagrams in order that a nuclear spin can be included This is illustrated in Figure 6 It is unnecessary to show the spin $|-\rangle$ state levels for two reasons they are well separated from the $|+\rangle$ spin state in relatively low fields because of the large magnetic moment of the electron and only transitions between muon states are important Accurate treatments cannot have this luxury [5]

In Figure 7 the two electron spin states have been considered, simply to demonstrate that only one of them will be involved in the level-crossing phenomenon In the case shown it is only the $|+\rangle$ state for $A_\mu > A_N$ which will show ALC resonance Conversely if $A_\mu < A_N$ it will be the $|-\rangle$ state Where the levels cross over the states both have the magnetic quantum number and, having the same Zeeman energy, the spins become indistinguishable and the states mix causing the levels to avoid each other as in Figure 8 However this enables a depolarising relaxation process at the level-crossing fields only which can be observed as was originally predicted by Abragam [3]

The advantages of the ALC technique are

1 Coupling constants of nuclei other than the muon can be measured
2 The precision is very high, as in ENDOR
3 There is a four-order increase in the allowed lifetime of the muon precursor since high longitudinal fields are used which conserves polarisation of the beam

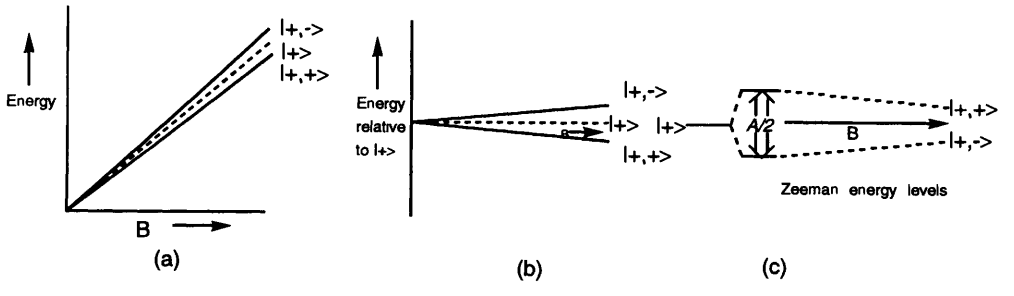

Figure 6 (a) Part of Figure 1 referring to electron spin state $|+\rangle$ only (b) Diagram (a) redrawn showing energies *relative* to electron spin state $|+\rangle$ (c) The effect of positive hyperfine coupling ($A > 0$) analogous to Figure 2

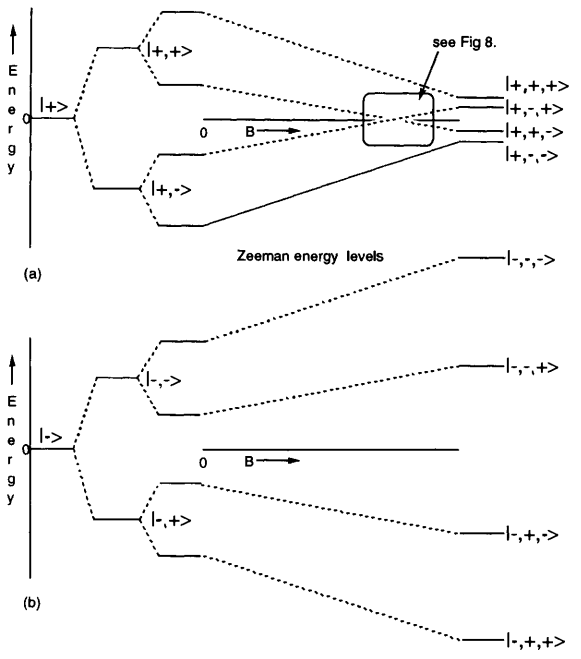

Figure 7 Levels associated with electron spin states for $A_\mu > A_N$: (a) $|+\rangle$; (b) $|-\rangle$. $|+\rangle$ refers to electron spin only, $|+,-\rangle$ refers to electron, muon spins only and $|+,-,+\rangle$ refers to electron, muon, nuclear spins. The energy is relative to the selected electron spin state.

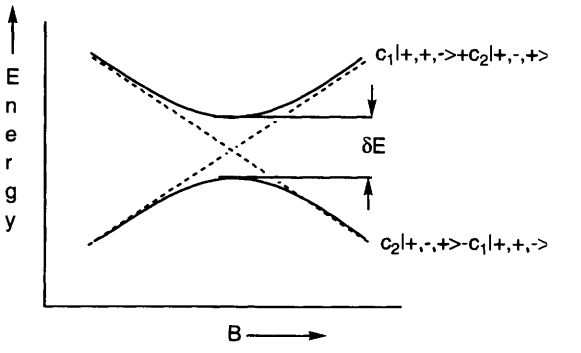

Figure 8 Avoidance of a level crossing. c_1 and c_2 vary with the magnetic field and are equal at the level crossing. $c_1^2 + c_2^2 = 1$.

4. The method is simpler than transverse-field experiments.
5. Larger muon fluxes, even muon pulses can be used.

The major disadvantage is that the entire field range of 3 T has to be scanned, searching for small resonances.

4.2 Closed-shell systems

Nuclear–electron interaction in *closed* shell molecules are dominated by the electron charge-nuclear charge interaction. This is the only possible electric interaction for electrons but nuclei can be more complicated and the point charge representation has to be modified for some (with spin angular momenta larger than ½) to include higher electric multipoles to account for asymmetries in the nuclear structure. The next possible multipole moment is the quadrupole, that is, the nuclear quadrupole moment. This interacts with electric field gradients (at its nucleus) which can arise from the charge distribution of the electron *density* mainly in the immediate neighbourhood of the nucleus. This will give rise to a manifold of nuclear quadrupolar energy levels. The level-crossing resonance technique, already briefly referred to with regard to hyperfine couplings of nuclei other than the muon, can be adapted to measure the electron electric field gradient–nuclear quadrupole moment interaction. By adjusting the external magnetic field strength the energy gap between the muon Zeeman levels can be matched to the magnetic levels of nuclei with quadrupole moments, determined mainly by the field-independent nuclear quadrupolar energy levels. Although detection of the resonance condition relies on their dipolar interaction, the quadrupole frequencies deduced from the spectrum enables identification and a measure of the electric-field gradient. Electric-field gradient calculations are not particularly difficult and are expected to have similar accuracy to that calculated for anistropic coupling constants for open-shell molecules in ESR since both a have a $1/r^3$ dependence. In both these cases the results are not unduly sensitive to the degree of electron correlation included in the wave function. For comparison the isotropic (Fermi contact) coupling constants, which require highly correlated wave functions, have been far more difficult to calculate reliably. The quadrupolar level-crossing resonance technique should produce results which are easier to model and interpret.

This extension of μSR into the realm of closed-shell molecules is more significant than just enabling identification of the elusive diamagnetic fraction. It is of course restricted to nuclei with nuclear quadrupole moments but good examples are ^{14}N (I = 1) and ^{17}O, the half integer spin (I = ½) actually facilitating detection of the resonance. The big disadvantage is that the muon must attach itself immediately adjacent to the atom with the quadrupole moment otherwise the effect will be severely attenuated.

5 Applications

5.1 Open-shell Systems

5.1.1 OMu

The proton derivative of the hydroxyl radical has been known over 30 years, being well characterised in the gas phase by Radford.[6] ESR has been less conclusive in condensed phases and no evidence has yet been obtained for the muon derivative, except possibly a loss of polarisation reflecting its existence, from μSR. This is unfortunate since it must be the simplest interesting radical having a one-dimensional potential energy hypersurface, that is, the variation of its energy with bond length, accurately represented by Morse-type potentials obtained from other spectroscopic means. The major problem is oxygen, which, being paramagnetic, induces a severe depolarisation of the muon before implantation and detection, which spoils the most obvious reaction:

$$Mu\cdot + O_3 \rightarrow OMu\cdot + O_2$$

It is not the oxygen produced in the reaction which is important but the oxgyen which accompanies the preparation of ozone itself. Ozone is also notoriously difficult to handle, particularly in the liquid or solid phase. There are other possible reactions which obviate this problem but the chosen reaction must be very fast if there is any chance of success. The importance of this molecule lies in its simplicity which illustrates many features of other more complicated molecules. A combination of results of *ab initio* theoretical calculations[7] and spectroscopic studies on this molecule will be used to illustrate the reasons why muonium substituted radicals are an important field of study.

Figure 9 describes the variation of the potential energy and electron–proton(muon) isotropic hyperfine coupling constant (a) for OMu near the equilibrium bond distance, r_e. The zero-point energies are indicated by horizontal lines (solid for the proton and dashed for the muon) with the associated probability distribution function for the corresponding zero-point motions. Before we continue a discussion of Figure 9 in detail some initial comments on the harmonic approximation of a chemical bond should be appreciated. The harmonic potential is symmetrical and the equilibrium bond length is the same as that averaged over any vibrational state. Hyperfine coupling constants which vary linearly, or as the cube, with change in bond length average over the zero-point motion to the same value as found for the equilibrium bond distance. Other functional variations, *e.g.* quadratic, will give observed coupling constants which depend on the nature of the vibration. If the potential is anharmonic, that is unsymmetrical, as expected in all bond-stretching vibrations, there will always be a change in the property

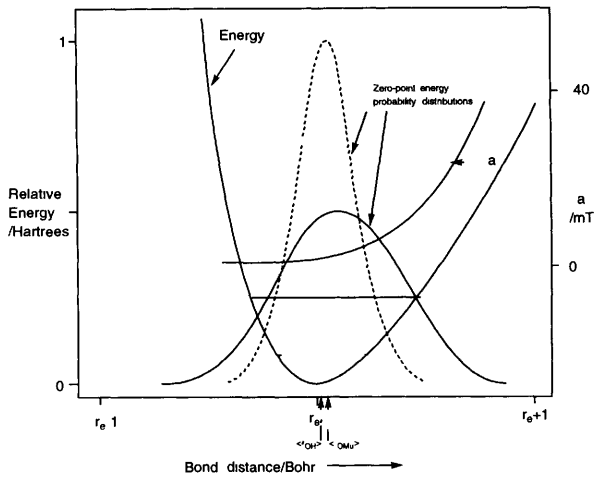

Figure 9 Energy, hyperfine coupling and zero-point motion in the hydroxyl radical

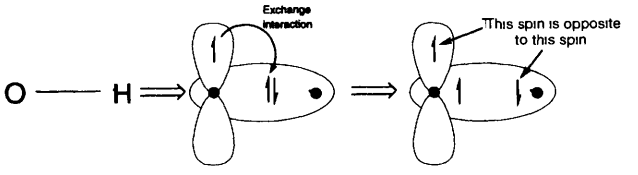

Figure 10 Qualitative explanation of negative spin density from spin polarisation mechanisms

at the equilibrium bond distance compared to that averaged over a vibration

This averaging process applies to other properties For example, the average bond length, after including the zero-point motion, of OH (*i e* $\langle r_{OH} \rangle$ in Figure 9) is lengthened by about 1 5% from the equilibrium bond distance, whereas the extension is close to 5% for OMu (*i e* $\langle r_{OMu} \rangle$) This is clearly a mass effect, the muon motion stretching far beyond the motion of the proton as shown by the zero-point energy distribution functions The height of each distribution function at each bond length is proportional to the time the molecule spends at that bond length The observed bond length is simply obtained by integrating the bond length times the height of the distribution function (suitably normalised) The asymmetry in the hydroxyl potential energy curve about the minimum energy position, as for all other diatomic molecules, is such that the curvature is much less for longer bond lengths Since the lighter muon samples a larger region from the minimum energy position to the proton its properties are much more sensitive to the anharmonicity Muonium chemistry therefore is a good method of probing large regions of potential energy hypersurfaces We can summarise as follows

If the bond closely approximates to a harmonic oscillator over its zero-point motion

1 the observed bond length is the same for all isotopes,
2 properties which vary linearly, or with a sigmoid shape centred about the optimum bond length, average to the same value as calculated at the optimum bond length

Any anharmonicity in the bond causes

1 the observed bond length to be larger for lighter isotopes,
2 change in all other properties no matter how they vary with bond length It is dangerous, although no doubt forms a good correlation, to assign properties calculated at the 'observed' bond length as an approximation to the value averaged over the zero-point motion

Every molecular isotopomer, within the Born–Oppenheimer approximation, shares the same potential energy hypersurface, for example, OH, OD and OMu share the same potential energy curve In addition any property which changes with molecular geometry will produce a similar property hypersurface which will be independent of isotopic substitution Experimental observation is simply a sampling of the property hypersurface according to the fraction of time that the molecule spends at each point In the case of hydroxyl the one-dimensional surface is sampled differently by each isotopomer as shown in Figure 9

The reduced hyperfine coupling constants, that is, $a = a_{obs} \times \mu_H/\mu_X$, where a_{obs} is the observed hyperfine coupling constant, and X is an isotope or pseudo-isotope of hydrogen with a magnetic moment μ_X, are listed in Table 1 If there was no residual isotope effect (hyperfine anomaly) the values should be the same for each potential function The effect, although significant for the harmonic potential, is considerably amplified if anharmonicity is allowed for

Note that the hyperfine coupling constants are calculated to be negative This can be rationalised with the help of Figure 10 The hydroxyl radical has an unpaired electron in a π-molecular orbital (effectively a p atomic orbital on the oxygen atom) A simple model places the proton or muon in the nodal plane of the p atomic orbitals and there is no hyperfine coupling as is the case with the electron pair in the chemical bond since both electrons behave identically, that is, their spin interactions with the proton will cancel out (no resultant spin density) The model can be extended to take into account the fact that the unpaired electron interacts with the two spin-paired electrons of the bond unequally as there is an exchange interaction (which effectively reduces the Coulomb repulsion) with the electron of like spin This increases the probability that the electrons of like spin will be closer than those of unlike spin, consequently spin-polarising the bond as indicated The proton or muon will therefore see more of the spin opposite to that in the p orbital on oxygen, giving rise to a negative spin density and correspondingly a negative hyperfine coupling constant As the bond stretches so the phenomenon will be enhanced leading to a rapidly increasing negative spin The asymmetry of the potential energy curve means that the muon samples the hyperfine couplings at long rather than short bond lengths which explains the significantly larger reduced hyperfine coupling constant of OMu compared to either OH or OD

5 1 2 The Ethyl Radical

β-Substituted ethyl radicals, CXH_2CH_2, have featured studies in the history of ESR spectroscopy[8] and naturally have attracted much attention in μSR spectroscopy Here the emphasis is two-fold, firstly, extending the discussion initiated with the hydroxyl radical, to illustrate typical vibrational modes which are to be expected with muonium adducts, and secondly discussing hindered internal rotation with regard to the unexpected effect of zero-point energies

5 1 2 1 Vibrational Modes

The light mass of the muon, typically leading to predicted stretching vibration frequencies of 9000 cm^{-1} from theoretical calculations, has been assumed to have its motion effectively decoupled from the rest of the molecule The temperature dependence of electron–muon hyperfine coupling constants, governed largely by low-frequency modes, will be discussed later but implies that decoupling the muon motion must be an approximation since the

Table 1 Reduced hyperfine coupling constants (a/mT) for isotopomers of the hydroxyl radical

Potential function/eV and how derived	OD	OH	OMu
UHF 5 1408[2 14($r_e - r$)]^2 (Harmonic approximation)	−1 276	−1 304	−1 490
UHF 5 1408{1 − exp[2 14($r_e - r$)]}^{2}	−1 348	−1 376	−1 717
Expt 4 624{1 − exp[2 293($r_e - r$)] − 0 0676($r - r_e$)exp[4 586($r_e - r$)][1 − 32 594($r_e - r$)]	−1 322	−1 348	−1 667

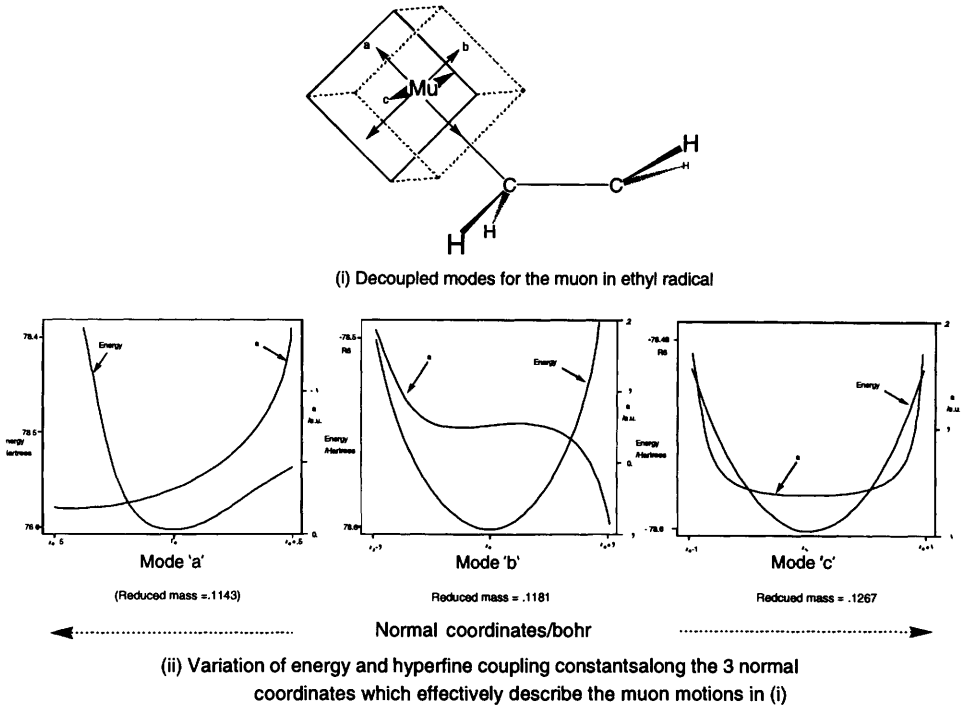

Figure 11 Simplified vibrations of the muon in CH_2MuCH_2 and their approximate association with the normal coordinates.

associated frequencies are far too high for more than the ground vibrational state to be populated. This part of the discussion is only concerned with molecules in their lowest vibrational state.

The decoupled motion of the muon in the ethyl radical is shown in Figure 11(i) directly along mutually orthogonal axes, one axis being coincident with the C–Mu bond (stretch vibration or mode 'a'), another right angles in the Mu–C–C plane (bend vibration or mode 'b') and the third perpendicular to the plane of the previous two (wag vibration or mode 'c'). It is clear that the stretch vibration [Figure 11(ii)] is quite different from the bend or wag in two ways: it is very anharmonic for large displacements from the minimum energy and the hyperfine coupling curve, a, has no symmetry. These two facts couple together to give a result analogous to that discussed for hydroxyl, and assigned to be largely responsible for the residual isotope effect, that is, the electron–muon reduced hyperfine coupling constant is larger than the equivalent proton coupling. The bend vibration is typically associated with the sigmoid shape curve [Figure 11(ii)] almost centred on the minimum energy position, which, because of the symmetric or harmonic appearance of the potential energy curve, contributes relatively little to the hyperfine coupling constant due to cancellations during averaging over the vibration. A large contribution may be expected from the wag mode since the coupling constant curve will make positive contributions over the whole range, that is, no cancellations. The similarity to the out-of-plane motion in the planar methyl radical, $\dot{C}H_3$, where the effect virtually accounts for half the observed coupling constant, is to be noted. However here the effect is small because the curve of the hyperfine coupling constant a is very flat over most of the zero-point motion and the contribution is again small.

5.1.2.2 Hindered Internal Rotation

In conformational analysis, groups of atoms attached across a single bond are described as two contra-rotating rigid groups. Since the potential energy will generally vary this is called a hindered internal rotation. The wag vibration [mode 'c' in Figure 11(i)] actually is coincident with an internal rotation of the whole CH_2Mu group relative to $\dot{C}H_2$ group about the C–C bond. In ethyl, $CH_3\dot{C}H_2$, the barrier to this rotation is unobservably small but in CH_2MuCH_2 it is about 3 kJ mol^{-1}.[9] This result initially attracted much attention. Hyperconjugation, possible when the C–Mu bond eclipses the unpaired electron orbital, when the two lie in the same plane on the same side of the molecule, was a possible explanation, being enhanced by the 'lengthening' of the C–Mu bond from anharmonicity. This result was important because it was related to an old area of research on similar radicals.

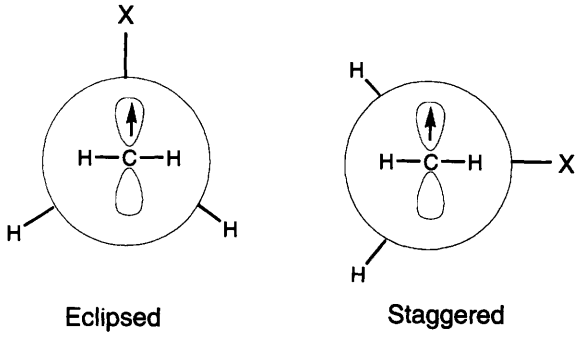

Figure 12 Conformations of β-substituted ethyl radicals.

There are two aspects which have to be considered: firstly the barrier to rotation and secondly the most stable site of the substituent X in CH_2XCH_2 as the projections in Figure 12 illustrate. The preference for deuterons (X = D) to take the staggered orientation[8] (340 kJ mol^{-1} lower than the eclipsed conformation) has to be contrasted with the 'eclipsed' preference of the corresponding proton in $CD_2H\dot{C}H_2$ and muon in CH_2MuCH_2 (376 and 2845 kJ mol^{-1} lower than the staggered conformation respectively). The mass difference, $m_X - m_Y$, for the radical CY_2XCH_2 is able to correlate

these results in two ways, the eclipsed conformation is preferred if $m_X < m_Y$ and the difference in energy between the conformations depends on the magnitude of the mass difference (assuming that the eclipsed conformation is slightly preferred if $m_X = m_Y$). Although zero-point energy effects were clearly indicated it was not obvious how this would explain the results Adding in the calculated contributions of the zero-point energy of all vibrations (in the harmonic approximation) except that coincident with the hindered internal rotations, an excellent correlation with experiment was found (see Table 2) This led to the development of an independent oscillator model, where the contributions of each atom in the molecule could be assigned a contribution proportional to $1/\sqrt{m}$, m being the nuclear mass The purpose of this exercise was to show that, within the harmonic approximation, the observation could be explained in terms of the force constant of each bond and how these varied during the hindered rotation. Any chemical interpretation of the effect would need to address this variation. Anharmonicity is not a necessary ingredient here but it can be anticipated to be important, particularly in the bond involving the muon, in two ways the asymmetry in the potential energy surface will affect the eclipsed–staggered conformational energy difference, and there will be a perturbation to the sampling of the surface by the other vibrations as well In Table 2 the conformational energy differences are consistently underestimated for the muon substituted radicals If the eclipsed position involves some enhanced hyperconjugative interaction the zero-point energy of the muon could be reduced further by anharmonicity which would lead to an increased energy difference, the hyperconjugative interaction being impossible in the staggered orientation In this way a chemical interpretation of the observations may be developed.

Table 2 Barrier height to hindered internal rotation in ethyl radical

Radical	Barrier height/J mol^{-1}		
	Experimental	Theory[10]	Independent oscillator model[11b]
CH_2DCH_2	−340[a]	−214	−714
CD_2HCH_2	376	319	376[c]
CH_2MuCH_2	2845	1875	2813

[a] Negative values indicate staggered conformation is more stable
[b] $-401 + 1558/\sqrt{m_X} - 1420/\sqrt{m_Y}$ Constant in oscillator model chosen to fit this value

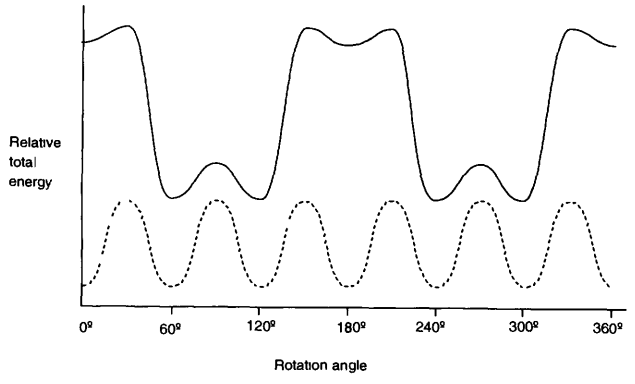

Figure 13 Relative total energy along the hindered rotation coordinate for *n*-propyl

This case is a good example where the potential energy hypersurface, including zero-point energy contributions, can completely change its shape by simply using different isotopes The effect is most clearly shown for CH_2DCH_2 in Figure 13 The dotted curve corresponds to the potential energy surface ignoring molecular vibration (also typical of the case for $m_X = m_Y$, as ethyl, CH_3CH_2 including zero-point energies), the solid curve includes the zero-point energy contributions from all vibrations except those along the hindered rotation coordinate The conformation at 0° is eclipsed which is at a higher energy than at 90° (staggered) If the corresponding curves had been presented for CH_2MuCH_2 the low-energy well would have appeared at 0° and the barrier at 90°, although 10 times higher

5 1 3 $C_{60}Mu$

The observation of $C_{60}Mu$ is always worthy of comment It is of interest here because of the cage structure *and* the fact that the next lightest atom is a factor of 54 times heavier than the muon which seemed to be a good example for studying the isotope effect. Two orientations of the optimised structure, from density functional calculations, of $C_{60}H$ are displayed in Figure 14, clearly illustrating the local distortion due to muonium addition The stretch, bend and wag motions are all analogous to those in Figure 11(i) and in this case were assumed to be normal coordinates [12] A hyperfine isotope effect, the percentage increase in the reduced coupling constant for the muon derivative compared to the proton derivative, was calculated to be 4% using harmonic potentials only and 6% including

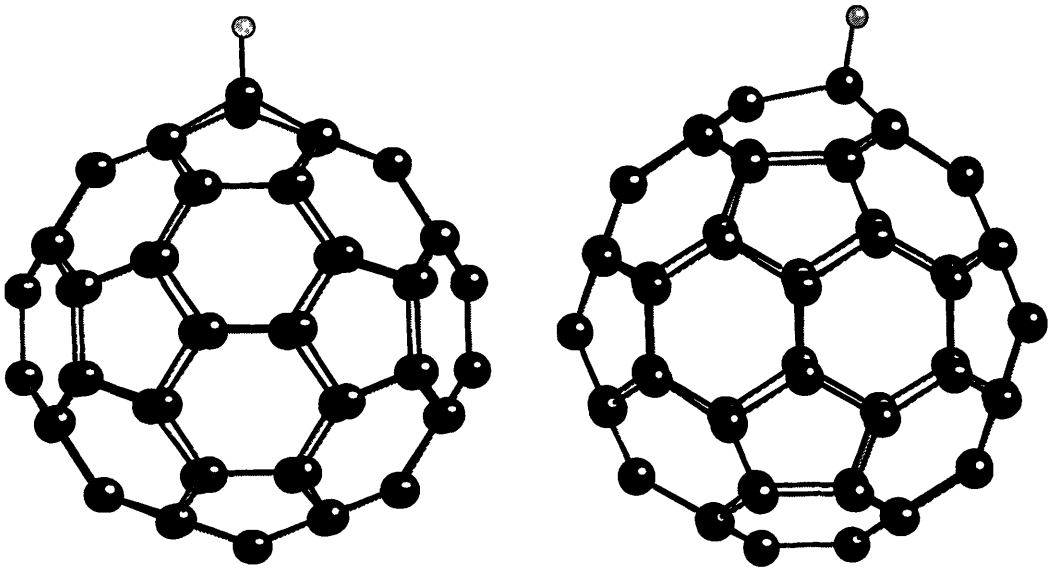

Figure 14 Structure of $C_{60}Mu$ (orientations differ by a 90° rotation about vertical)

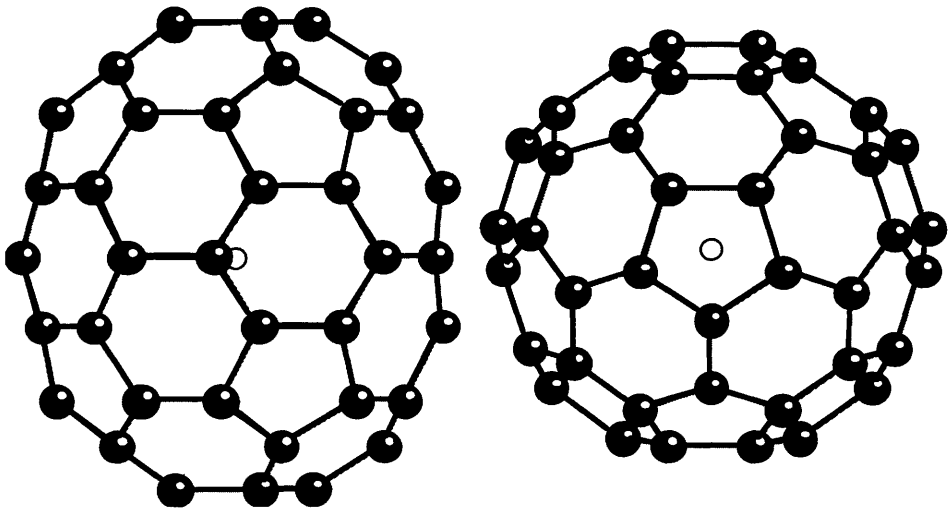

Figure 15 Two orientations of $Mu@C_{70}$. Left is long axis vertical. Right is long axis perpendicular to paper. The muon is the lighter shaded atom and not bonded by any other atom.

anharmonicity. The experimental value is about 9%.[13] The value for just the stretch vibration, including anharmonicity, was 5%. The discrepancy of 3% seemed quite reasonable since there must be contributions from other modes. The necessity to invoke anharmonicity in the molecular vibrations has been questioned[14] using semi-empirical calculations which are known to give a more delocalised distribution of the unpaired electron than current *ab initio* calculations. These semi-empirical results certainly may account for the experimental results better but if anharmonic contributions are included some amplification of the effect is anticipated so presumably semi-empirical calculations overestimate the hyperfine anomaly, although any conclusion for such a large molecule should be treated with extreme caution. It must not be forgotten that the replacement of a proton with a muon will affect all the vibrational modes, a complication for all except diatomic radicals. This makes the observation of OMu even more crucial.

5.1.4 $Mu@C_{70}$

C_{70} is much more interesting than C_{60} since three different exohedral $C_{70}Mu$ radicals have been characterised with relatively small hyperfine coupling constants (*ca.* 300 MHz) reflecting the fact that the carbon atoms in C_{70} are not all chemically equivalent. There are five different types of carbon atom in C_{70}, but it is possible that the band of hexagens around the equator (perpendicular to the long axis, see Figure 15) are more aromatic than those at the poles and hence have a reduced probability of forming a bond to muonium. Analogous to C_{60} ($Mu@C_{60}$) there is also an endohedral radical, $Mu@C_{70}$, where the hyperfine coupling constant is close to the free muonium value. It is generally agreed that in both the endohedral radicals the muonium is not specifically bonded to the cage and in $Mu@C_{60}$ is oscillates in a symmetrical potential energy well at the centre, in accordance with the isotropic nature of the hyperfine coupling constant. $Mu@C_{70}$ differs in that there is a small but detectable anisotropic coupling constant ($2B$ = 1.02 MHz).[15] Assuming there is no breakdown of the Born–Oppenheimer approximation there are at least three interpretations:

1. the average position of the endohedral muonium is *not* at the centre;
2. the vibrational motion is anisotropic about the centre;
3. the muonium orbital is distorted by interaction with the fullerene cage when at the centre.

Ab initio calculations[16] confirm that there is a metastable site near the centre with the expected large hyperfine coupling constant if the cage is not allowed to distort. Bonding to the inside of the cage will result in the muon being permanently trapped due to the associated cage distortion and was not considered further. Significantly the centre of C_{70} does not correspond to an energy minimum; it is a saddle point (see Figure 16). Although there is a minimum along the long (z) axis at the centre it is only a shallow minimum and deeper minima are found about 1.5 Å from the centre. Along the short axes no minima are observed at the centre but occur about 1 Å radially from the centre in the equatorial plane. The volume bounded by these deep minima is close to an ellipsoid and we can imagine the muonium being trapped in an ellipsoidal shell potential well sharing a common centre and a common long axis with C_{70}. Within this ellipsoidal well the isotropic coupling constant remains close to the free muonium value. If muonium can access the whole of the volume in the ellipsoidal shell then the average position of the muonium will be at the centre, even though the probability of finding it there will be low.

By symmetry a p orbital at the centre of C_{70} cannot mix in with the 1s orbital, which must be the dominant component of the orbital on muonium to give the free muonium hyperfine coupling constant, but d orbitals can. Since there is not a true minimum at the centre in any case there is no reason why p orbitals should not mix in with the 1s orbital in all parts of the ellipsoidal shell. However the contributions to the anisotropic coupling constant are not all additive.

Certainly a freely moving muonium in this shell will be equivalent to an anisotropic vibrational motion and this gives a value $2B = -0.08$ MHz. This is a factor of 10 too small and some hindrance to the motion should be included but an explanation of the original observation has been provided. If the muonium should be trapped, or spend the major part of its time in the wells on the z axis, values of $2B$ larger than experiment are predicted.

5.2 Closed-shell systems

Quadrupolar level-crossing resonance is used for all the examples. The existence of an electric field gradient at an quadrupolar nucleus can normally be expected to exist, except for perhaps NH_3Mu^+. But even here the inclusion of the zero-point motion shows that the symmetry is broken by the mass difference of the muon relative to the protons. The effect is small; it is estimated that the field required in the muon level-crossing resonance experiment should be as low as 3 Gauss (1 G = 10^{-4} T), a challenging, if not impossible, experiment. The feature of the calculations[17] on HCl and MuCl suggests

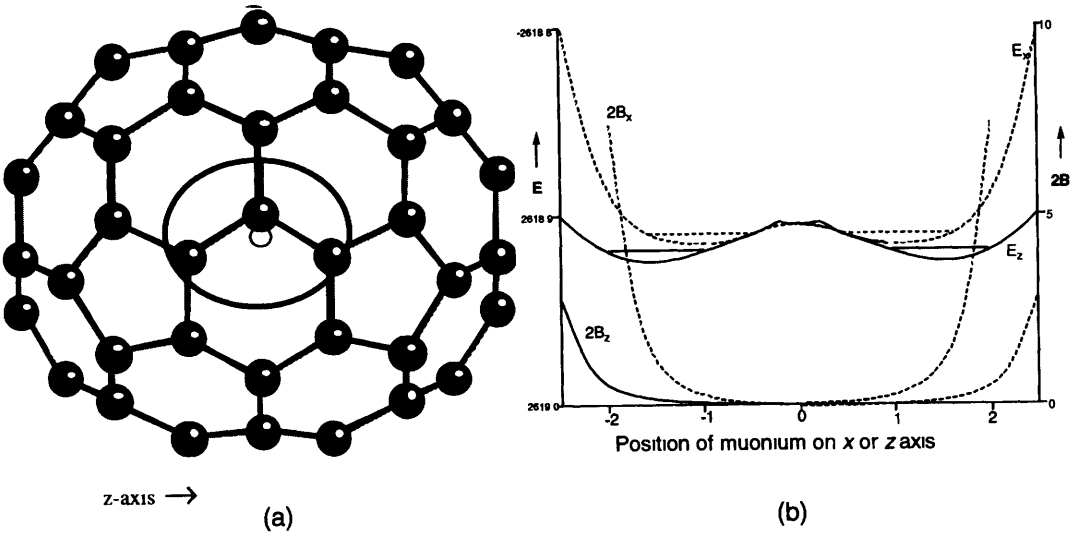

Figure 16 (a) Elliptical contour of minimum energy (b) Variation of energy and $2B$ along principal axes

that the isotope effect (from the zero-point motion) is only 2%, due to an unexpected[18] cancellation of the harmonic and anharmonic contributions, whereas the calculated (free molecule) quadrupole constant (58 MHz) does not compare well with the NQR value (68 MHz) in the solid

5 2 1 Complex with N_2

Ever since the accidental discovery[19] of a spectrum assigned to N^2H^+ from interstellar emissions the ion has been the subject of many experimental and theoretical investigations A nitrogen quadrupole interaction of 2 26 MHz was measured[20] from ALC μSR spectra at 37 K and it was proposed that this was due to N_2Mu^+ This was curious since values of -5 7 MHz from N_2H^+ measurements had been quoted with calculated values of the electric-field gradients at the nitrogen furthest from the proton giving -5 3 MHz and at the nitrogen adjacent to the proton giving -1 2 MHz The possibility of a large vibrational isotope was certainly considered to be a possibility as well as the effects of the crystalline environment It is expected that the nitrogen adjacent to the muon will be dominant in the ALC μSR spectrum In view of the smallness of the ion triple-zeta-quality basis orbitals including polarisation functions on all atoms were used to study the linear molecular cation $[N_2MuN_2]^+$ (Table 3) [21]

The nitrogen atoms adjacent to the muon clearly give acceptable values to explain the observed coupling constants Further encouragement comes from the reaction (X = H or Mu)

$$N_2X^+ + N_2 \rightarrow [N_2XN_2]^+ \qquad \Delta E_H = -83 \text{ kJ mol}^{-1} \text{ and } \Delta E_{Mu} = -99 \text{ kJ mol}^{-1}$$

Table 3 Quadrupole coupling constants (χ/MHz) of the nitrogen nuclei of $[N_2MuN_2]^+$ The atoms are labelled from left to right in the molecule N–N–Mu–N–N as 1–2–Mu–3–4 MP2 are second-order Møller-Plesset calculations, QCISD are quadratic configuration interactions including all single and double replacements in the Hartree-Fork reference determinant and DFT are density functional theory calculations

Method	χ_{zz} (N_1)	χ_{zz} (N_2)	χ_{zz} (N_3)	χ_{zz} (N_4)
MP2	−4 363	−2 297	−2 297	−4 363
QCISD	−4 898	−2 462	−2 462	−4 898
DFT	−5 026	−2 411	−2 411	−5 026

which implies that not only is the cation more stable than its components, but that the muon derivative is more stable than the proton derivative This is surprising since the number of vibrational modes contributing to the total zero-point energy is 10 for $[N_2MuN_2]^+$ but only 5 exist for the reactants N_2 and N_2X^+ The replacement of a very strong bond (N–X) by two very weak bonds can significantly decrease the zero-point energy, an effect which increases in importance the lighter the mass of X The calculated increase in quadrupole coupling constant between the proton and the muon due to vibrational averaging is calculated to be less than 2%, which is not significant

5.2 HOMu in Ice

Larger changes in the ^{17}O quadrupole coupling constants are suggested from ALC μSr data in ice with reported[22] values of 6 1 MHz, η = 1 (dimensionless asymmetry parameter), compared with NQR results for normal ice (6 41 MHz, η = 0 93 at 77 K) and D_2O ice (6 66 MHz, η = 0 94), implying isotope reductions of the order of 4% for the muon pseudo-isotope These results are to be compared with HDO results (10 17 MHz, η = 0 75) in the gas phase Webster[23] studied theoretically the potential energy surface of isolated H_2O and used it to determine a zero-point vibrational correction to the ^{17}O nuclear quadrupole coupling constant of a series of isotopomers, including MuOH It was noted that the isotope shift resulting from muonium substitution is in the opposite direction relative to the corresponding deuterium shift when comparing theory and experiment Of course the effects of hydrogen bonding are known to be very important in ice and recent calculations[24] on two clusters of 27 water molecules (see Figure 17) confirm this One of the difficulties in studying ice are the large number of possible hydrogen-bonded structures The structures of the clusters are chosen since they display a plane of symmetry

The vertical bonds are different to the other bonds due to the wurtzite structure and these two structures make use of that bond differently Calculations of 7 4 MHz for the quadrupole coupling constant compare well with NQR results of 6 4—6 7 MHz Since the best results of Webster for isolated molecules exceed the gas-phase HDO values by 13%, we note that reducing the calculated ice value by 13% gives 6 5 MHz, well within the experimental range The next step is to allow for some vibrational motion, particularly the muon, and try to get a lowering of the quadrupole coupling constant of the adjacent oxygen This would certainly add a considerable weight of evidence to the assignment already made [22]

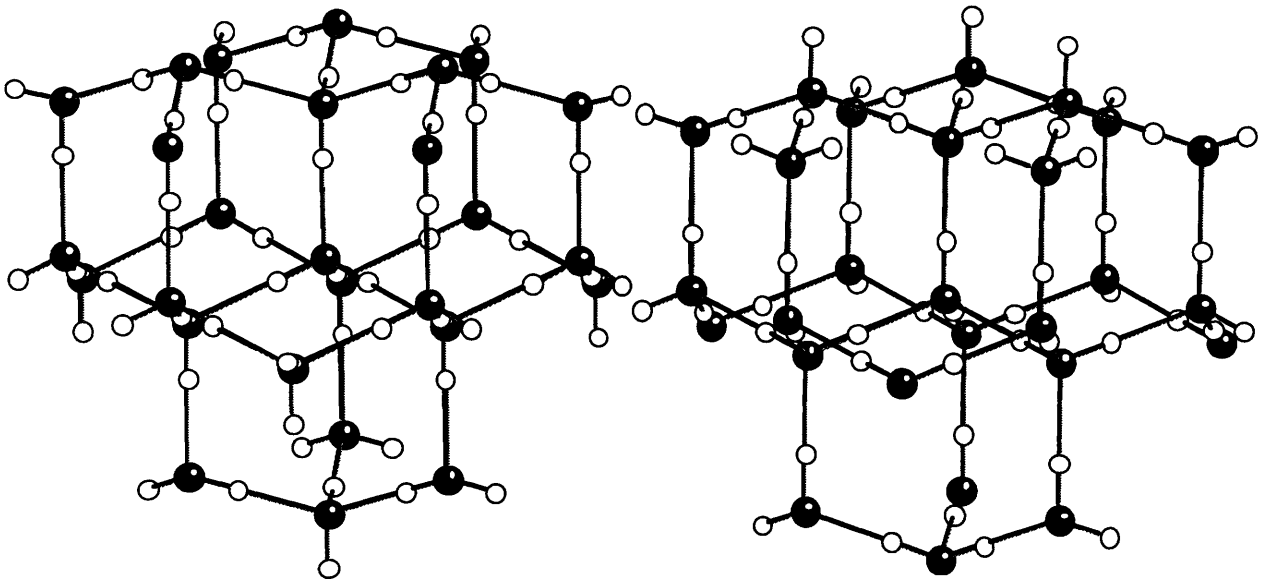

Figure 17 Two clusters of 27 water molecules chosen to preserve a plane of symmetry.

6 Thermodynamic and Kinetic Stability

Before the rate of a chemical reaction is studied the mechanism must be proved beyond reasonable doubt. This applies to muon studies as much as in any other branch of chemistry. In view of the low concentration of muon species any reaction initiated by muons or muonium will hardly be complicated by competing reactions with products *etc*. We will look at a few examples to illustrate the interesting aspects of experiments with muons as well as the pitfalls.

6.1 Addition to Pyrazine

Figure 18 describes the two possible products for the addition reaction to pyrazine. Experimentally muonium adds to carbon[25] in

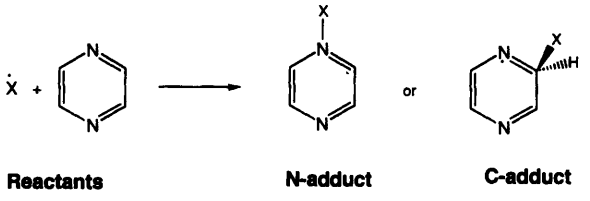

Figure 18 Reaction of pyrazine with pseudo-isotope or isotope of hydrogen, X.

pyrazine whereas protium (hydrogen atom) adds to nitrogen.[26] It appears that this could be an interesting observation which chemically differentiates between muonium and protium. If the mechanism involves muonium or protium, in the absence of solvation effects, simple considerations based on the disruption of the system clearly shows a preference for the C-adduct as the most stable radical. The residue of the disrupted π-system of the C-adduct (Figure 19) involves two electronegative N atoms whereas the N-adduct involves just one and therefore the C-adduct should be thermodynamically more stable. This explains the result of the

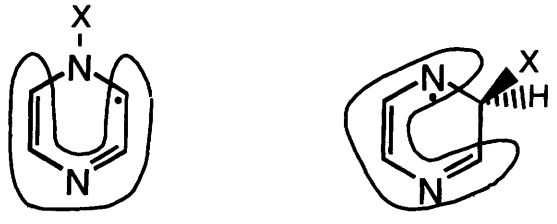

Figure 19 Disruption of the pyrazine π-system on muonium addition.

muonium addition. Confirmation of this qualitative argument using *ab initio* UHF calculations[27] has not been forthcoming since the N-adduct was calculated to be the most stable. However a study of the transition states of both adducts led to the conclusion that the C-adduct will be favoured kinetically, and would not be affected by the mass of the attacking atom, muonium or protium. The problem remaining is 'Why does protium form the N-adduct?' The answer is 'mechanism': the protium N-adduct is formed in acid solution where hydrogen ions are in high concentration and will tend to protonate a lone pair of electrons on nitrogen to form the cation of the N-adduct which subsequently picks up an electron, a two-stage process. The muonium adduct presumably is formed by a one-stage process, that is, the two adducts are formed *via* different mechanisms. If this is so, and it seems to be the case, comparisons of reaction rates are not so interesting. However the story does not end there. Further *ab initio* calculations using the same basis set as the UHF calculations but carried out within the framework of Density Functional Theory (DFT) and second order Møller-Plesset perturbation theory (MP2) methods[28] conclude that the C-adduct is more thermodynamically stable as the original qualitative argument implied and obviates the necessity to resort to a study of transition states. Disturbingly (see Table 4) the DFT calculations suggest that both muonium adducts are unstable once the zero-point energy is included.

6.2 Instability of MuCO relative to HCO

HCO is a well known product from flash photolysis of acetaldehyde and can also be made by the reaction of hydrogen atoms (from photolysis of HI) with carbon monoxide. The formation of MuCO from muonium should be an excellent prospect. Unfortunately although no experiment has conclusively obtained a signature for MuCO nor its hyperfine coupling constants, two observations[29] have inferred its existence: the unusual temperature dependence in a transverse-field μSR experiment using dilute mixtures of CO in N_2 and the muon spin relaxation in longitudinal fields. The obvious interpretation is that MuCO must be unstable.

To investigate this proposition *ab initio* calculations[30] on the potential-energy surface were carried out using methods which incorporate electron correlation: density functional methods (DFT) using two different functionals, up to fourth-order Møller-Plesset perturbation (MPn, n = 2,3,4) theory and quadratic configuration interaction including all single and double replacements and triples by perturbation theory [QCISD(T)]. The results for the QCISD(T) calculations are shown in Figure 20 and are quite similar to those for all other calculations except DFT. All agree that COX structures

Table 4 Internal energy changes after reaction of pyrazine and hydrogen or muonium The ROHF and UHF values are both derived from the RHF calculations on pyrazine and ROHF calculations on hydrogen The zero-point energies from the DFT calculations on the adducts have been used to estimate ΔE(MP2)

	ΔE (Change in internal energy/kJ mol $^{-1}$)							
	ROHF		UHF		DFT		MP2	
Reaction	ΔE_H	ΔE_{Mu}	ΔE_H	ΔE_{Mu}	ΔE_H	ΔE_{Mu}	ΔE_H	ΔE_{Mu}
$X + C_4H_4N_2 \rightarrow N - adduct$	−60	0	−118	−72	+265	+327	−1742	−1696
$X + C_4H_4N_2 \rightarrow C - adduct$	+5	+63	−52	−12	−7	+50	−2025	−1968

(X = H or Mu) are less stable than XCO The crucial reaction is therefore

$$X + CO \rightarrow XCO$$

and the associated energy change ΔE_X (Table 5) *Positive* values indicate that the product is unstable compared to the reactants The DFT results were rejected as spurious since the results were at variance also with ROHF (restricted open-shell Hartree-Fock)

Table 5 Energy change in Hartrees for the reaction X + CO → XCO for various theoretical methods

Method	ΔE_H	ΔE_{Mu}
MP4	−0 012617	+0 003025
DFT(BLYP)	−0 030854	−0 016003
DFT(SVWN)	−0 044826	−0 029787
QCISD(T)	−0 012026	+0 003982

and UHF (unrestricted HF) methods, identifying a possible problem with the functionals when comparing a singlet-state energy of CO with the doublet-state energy of HCO Apart from this difference the proposition that the increased zero-point energy of muonium substitution compared to protium is sufficient to make the product unstable is verified and explains the peculiar temperature dependence in transverse fields The fast muon relaxation observed in high fields has been associated with equilibria of the type

$$OC{-}MuCO \leftrightarrow OCMu \quad \text{or} \quad CO{-}MuCO \leftrightarrow COMu{-}CO$$

Also, in fields of a few kilogauss, as usually employed, the μSR spectrum is likely to involve frequencies in excess of 500 MHz

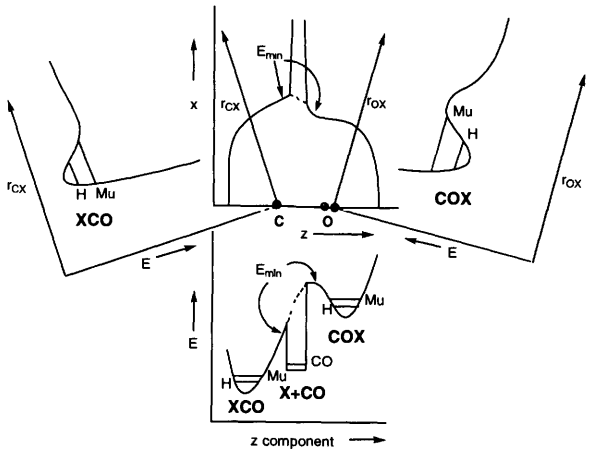

Figure 20 Some potential energy surfaces of the complex involving X (H or Mu) and CO from QCISD(T) calculations ● denotes the positions of the C and O atoms for the COX radical For XCO the CO bond length is shorter and the position of O is represented by ● The bottom diagram follows the energy of the minimum energy contour (E_{min}, top diagram) plotted against the z component The other two diagrams are bond length/potential energy diagrams for the CX and OX bonds The lines labelled H, Mu or CO are appropriate zero point energies

which are difficult or impossible to detect for short-lived radicals which undergo fast spin relaxation

7 Closing Comments

The light mass of the muon and the pseudo-isotopic nature of muonium with all the armoury from its decay process has already opened the opportunity to look into molecular processes which seemed impossible a short time ago There are many areas, such as semi-conductors, not easily placed into the chemistry category where its influence has been even more startling Looking back to the 1950s the muon, even muonium, was to a chemist, to put it bluntly, just another physicists play-thing In the 1960s, to a chemist, it was still science fiction but might have been in danger of achieving the status of crank science in the 1970s New sources of muons (and a better public relations effort) raised its profile over the next decade to (debatably) 'state of the art', until in the 1990s it has been established as a useful tool, although for the very few Over the same period mainframe computers have been reduced to portables and NMR spectrometers, transformed from the specialist physics laboratory, have ended up under the domination of organic chemists Are μSR spectrometers destined to be tied to giant accelerators in as many places round the world as can be counted on the fingers of both hands?[31]

Another way of quantifying the development of μSR is to look at the quantities of material required for an experiment, which can be crucial to a chemist Enormous (> 100 g) aliquots were necessary to stop the muons in the 1960s, but this was reduced to a few grams by the mid-1970s Surface muons require only about 50 milligrams and this was achieved 10 years ago Techniques such as phase-space compression and 'cooled' muons are expected to reduce the amount to less than a milligram in the next year or so Microgram quantities are envisaged using the technique of regenerating muons by ionising muonium, but give that another 10 years

For chemistry the future, although polarised, is bright

8 References

1 S F J Cox, *J Phys C Solid State Phys*, 1987, **20**, 3187
2 E Roduner, *Lecture Notes in Chemistry*, Springer-Verlag, 1988, vol 49, *Chem Soc Rev*, 1993, **22**, 339
3 A Abragam, *Compt Rend Ser II*, 1984, **299**, 95
4 E Roduner, P L W Tregenna Piggott, H Dilger, K Ehrensberger and M Senba, *J Chem Soc Faraday Trans*, 1935, **91**, 1935
5 M Heming, E Roduner, B D Patterson, W Odermatt, J Schneider, H Baumeler, H Keller and I M Savic, *Chem Phys Lett*, 1986, **128**, 100
6 H E Radford, *Phys Rev*, 1961, **122**, 114
7 T A Claxton, A M Graham, S F J Cox, Dj M Maric, P F Meier and S Vogel, *Hyperfine Int*, 1990, **65**, 913
8 R W Fessenden, *J Chim Phys*, 1964, **61**, 1570
9 M J Ramos, D McKenna and B C Webster, *J Chem Soc Faraday Trans 1*, 1984, **80**, 267
10 T A Claxton and A M Graham, *J Chem Soc Chem Commun*, 1987, 1167
11 T A Claxton and A M Graham, *J Chem Soc Faraday Trans 2*, 1988, **84**, 121
12 M A Boxwell, T A Claxton and S F J Cox, *J Chem Soc Faraday Trans*, 1993, **89**, 2957
13 J R Morton, K F Preston, P J Krusic and L B Knight Jr, *Chem Phys Lett*, 1993, **204**, 401

14 J. R. Morton, F. Negri and K. F. Preston, *Phys. Rev. B*, 1994, **49**, 12446.
15 K. Prassides, T. J. S. Dennis, C. Christides, E. Roduner, H. W. Kroto, R. Taylor and D. R. M. Walton, *J. Phys. Chem.*, 1992, **96**, 10600.
16 T. A. Claxton, *Phil. Mag., B*, 1995, **72**, 259.
17 T. A. Claxton and S. F. J. Cox, *Hyp. Int.*, 1994, **87**, 917.
18 This contrasts with the *hyperfine* isotope effect for β-protons and muons in organic radicals where the corresponding terms reinforce each other.
19 B. E. Turner, *Astrophys. J.*, 1974, **193**, L89.
20 V. Storchak, G. D. Morris, K. Chow, W. N. Hardy, J. H. Brewer, S. R. Kreitzman, M. Senba, J. W. Schneider and P. Mendels, *Chem. Phys. Lett.*, 1992, **200**, 546.
21 T. A. Claxton, *Phil. Mag., B*, 1995, **72**, 251.
22 S. F. J. Cox, G. H. Eaton, J. E. Magraw and C. A. Scott, *Chem. Phys. Lett.*, 1989, **160**, 85.
23 B. C. Webster and D. Buttar, *J. Chem. Soc., Faraday Trans.*, 1992, **88**, 087.
24 T. A. Claxton and T. G. Pawson, unpublished.
25 Z. Wu, M. V. Barnabas, J. M. Stadlbauer, K. Venkateswaran, G. B. Porter and D. C. Walker, *J. Am. Chem. Soc.*, 1991, **113**, 9096; B. L. Baron and G. F. Fraekel, *J. Chem. Phys.*, 1964, **41**, 1455.
26 B. L. Baron and G. F. Fraenkel, *J. Chem. Phys.*, 1964, **41**, 1455; H. Zeldes and R. Livingston, *J. Phys. Chem.*, 1972, **76**, 3348.
27 R. Gelabert, M. Moreno and J. M. Lluch, *J. Phys. Chem.*, 1994, **98**, 7858.
28 T. A. Claxton and I. M. Smith, *J. Phys. Chem.*, 1995, **99**, 13301.
29 D. M. Garner in 'TRIUMF Annual Report on Scientific Activities', 1985, r. 55; J J. Pan, D. G. Fleming, M. Senba, D. J. Arsenau, R. Snooks, S. Baer, M. Shelley, P. W. Percival, J.-C. Brodovitch, B. Addison-Jones, S. Wlodek and S. F. J. Cox, *Hyp. Int.* 1994, **87**, 865.
30 T. A. Claxton and S. F. J. Cox, *Phil. Mag., B*, 1995, **72**, 267.
31 Ivan Reid, PSI, Switzerland has privately estimated a desk-top μSR spectrometer would only cost $20 000 000.